Expedition 301 synthesis: hydrogeologic studies[1]

A.T. Fisher[2]

Chapter contents

[1] Fisher, A.T., 2009. Expedition 301 synthesis: hydrogeologic studies. *In* Fisher, A.T., Urabe, T., Klaus, A., and the Expedition 301 Scientists, *Proc. IODP,* 301: College Station, TX (Integrated Ocean Drilling Program Management International, Inc.). doi:10.2204/iodp.proc.301.206.2009
[2] Earth and Planetary Sciences Department and Institute for Geophysics and Planetary Physics, University of California, Santa Cruz CA 95064, USA. **afisher@ucsc.edu**

Abstract

Integrated Ocean Drilling Program Expedition 301 was part of a long term series of operations and experiments focused on quantifying hydrogeologic, lithologic, biogeochemical, and microbiological properties, processes, and linkages in basaltic crust on the eastern flank of the Juan de Fuca Ridge. This paper summarizes peer-reviewed hydrogeologic studies published since the end of Expedition 301. Regional survey data show that patterns of fluid circulation in basement on this ridge flank are complex, including components of fluid flow in the ridge-parallel (along-strike) direction. Numerical models show that hydrothermal circulation can form a hydrothermal siphon between recharging and discharging basement outcrops that penetrate regionally thick sediments, provided basement permeability is $\geq 10^{-12}$ m^2. Simulated fluid temperatures in upper basement between outcrops are consistent with observations (60°–65°C) if large-scale basement permeability is ~10^{-11} m^2. Other models show that basement conditions in the Expedition 301 field area may be undergoing thermal rebound following the end of an earlier phase of open hydrothermal circulation that extracted a larger fraction of lithospheric heat than is extracted today. This hypothesis is consistent with trends in basement geophysical properties, as determined with Expedition 301 wireline logs and tests on core samples from upper basement, which suggest that upper basement has not been warmer than it is at present. Drill string packer experiments in upper basement during Expedition 301 indicate a layered crustal structure, with bulk permeabilities from 10^{-12} to 10^{-11} m^2. Additional hydrogeologic analyses were completed using the formation pressure response to the long-term flow of cold bottom seawater into basement at Site U1301 during 13 months after drilling, as observed at Site 1027 (2.4 km away). These analyses suggest large-scale permeability at the low end of values indicated by packer testing, 0.7×10^{-12} m^2 to 2×10^{-12} m^2. Results from these two sets of measurements, and the difference between these permeability estimates and others based on modeling and analyses of formation responses to tidal and tectonic perturbations, may be reconciled if the upper crust in this area is anisotropic with respect to basement permeability. This hypothesis will be tested during and after the next drilling expedition in this area, when multidirectional crosshole experiments are run using a network of sealed borehole observatories.

doi:10.2204/iodp.proc.301.206.2009

Introduction

Integrated Ocean Drilling Program (IODP) Expedition 301 was part of a series of expeditions and experiments to quantify hydrogeologic, lithologic, biogeochemical, and microbiological properties, processes, and linkages on the eastern flank of the Juan de Fuca Ridge. This effort included site surveys to map bathymetric relief, seismic reflection profiles to delineate sediment thickness, sediment cores to allow analysis of pore fluids, and heat flow measurements to determine patterns of lithospheric and hydrothermal heat loss. Operations during Expedition 301 included replacing one existing subseafloor borehole observatory (CORK), drilling two basement holes and installing two new long-term observatories, coring the upper ~300 m of basement and shallow sediments above basement, and collecting in situ hydrogeologic and geophysical data from basement. Subsequent remotely operated vehicle (ROV) and submersible expeditions have serviced IODP observatories, collecting pressure and temperature data and fluid and microbiological samples and replacing components as needed to maintain these systems for future use. Another drilling expedition is planned to emplace three more borehole observatories (one in an existing basement hole and two in new holes) and initiate crosshole tests, and additional ROV and submersible expeditions will conduct long-term experiments and recover subseafloor data and samples. Proposals and planning for work that eventually led to Expedition 301 began in 1998, and completion of long-term experiments will require 3–4 y after the second drilling expedition. Thus Expedition 301 was part of a long-term effort, likely to last 15–16 y in total.

This paper summarizes operations and scientific studies related to Expedition 301 and having an emphasis on the hydrogeology of upper ocean crust. These studies have helped to advance high-priority goals that motivated Expedition 301, although completion of the main crosshole experiments will occur during and after the next drilling expedition. Other research papers published since the end of Expedition 301 include studies of sedimentology (Kiyoka and Yokoyama, submitted), physical properties (Goto and Matsubayashi, 2008), fluid geochemistry (Wheat and McManus, 2008), sedimentary microbiology (Engelen et al., 2008; Lipp et al., 2008; Nakagawa et al., 2006), contamination during coring (Lever et al., 2006), and methods in organic geochemistry (Heuer et al., 2006). A comprehensive listing of publications associated with Expedition 301 can be found at **publications.iodp.org/proceedings/301/301bib.htm.**

Regional studies, prior drilling, and modeling of the Expedition 301 area

Earlier studies summarize the geological, survey, and drilling history of the Expedition 301 area and surrounding region in detail (Davis et al., 1992, 1997; Davis and Currie, 1993; Hutnak et al., 2006; Rosenberger et al., 2000; **Zühlsdorff et al.**). The eastern flank of the Juan de Fuca Ridge near 48°N has some features common to ridge flanks in general, including extrusive igneous basement overlain by sediments that thicken with crustal age and abyssal hill topography bounded by high-angle faults, forming linear structural trends that run subparallel to the spreading ridge to the west (Fig. **F1**). However, turbidites that flowed from the nearby North American continent in the Pleistocene blanketed the crust in the Expedition 301 area with thick sediments at an unusually young age. Basement rocks remain exposed over large areas mainly close to the active spreading center, and seamounts and smaller basement outcrops also occur up to 100 km east of the spreading center, especially to the north and south of the Expedition 301 work area (Fig. **F1**).

Operations during Ocean Drilling Program (ODP) Leg 168 completed a drilling transect of eight sites across 0.9 to 3.6 Ma seafloor; collected sediment, rock, and fluid samples; determined thermal, geochemical, and hydrogeologic conditions in basement; and installed a series of CORK observatories in the upper crust (Davis, Fisher, Firth, et al., 1997). Two of the Leg 168 observatories were placed in 3.5–3.6 Ma seafloor near the eastern end of the drilling transect, in Holes 1026B and 1027C (Fig. **F1**). Expedition 301 returned to this area and drilled deeper into basement; sampled additional sediment, basalt, and microbiological materials; replaced the borehole observatory in Hole 1026B; and established two multilevel observatories at Site U1301 for use in long-term, three-dimensional hydrogeologic experiments (see the **"Expedition 301 summary"** chapter).

Several studies prior to Expedition 301 explored locations where hydrothermal fluids discharge, recharge, or flow laterally through basement. Before Leg 168, there was a mostly two-dimensional view of the dominant fluid circulation pathways in this area, with recharge occurring across large areas of base-

ment exposure close to the ridge (near the western end of the Leg 168 transect) (Fig. F1A), then flowing toward the east. Some results from Leg 168 were consistent with this view, including seafloor heat flow and basement temperatures that increased and basement fluids that were warmer and more altered with greater distance to the east along the drilling transect (e.g., Davis et al., 1992, 1999; Davis, Fisher, Firth, et al., 1997; Elderfield et al., 1999). But there were inconsistencies with this conceptual model of large-scale hydrogeologic flow, especially after Leg 168 results were considered. For example, although basement fluids warmed and aged along the western end of the Leg 168 drilling transect with increasing distance from the ridge (from Site 1023 to Site 1025), fluids were younger with respect to ^{14}C at the next nearest site to the east (Site 1031) and younger still farther to the east (at Site 1026) (Fig. F1A), despite being warmer and more altered (Elderfield et al., 1999). In addition, reexamination of existing bathymetric data and collection of additional data along western end the Leg 168 transect showed basement outcrops to the north and south that could allow hydrothermal fluids to recharge and discharge, with flow occurring nearly perpendicular to the transect (Hutnak et al., 2006). There was also the vexing problem of explaining where fluids flowing toward the east at the western end of the Leg 168 transect might exit the crust (e.g., Davis et al., 1999). It is not possible for large volumes of fluid to recharge the crust, flow laterally across tens of kilometers, and then be stored indefinitely. In fact, discharge is required as a complement to recharge in order for a flow system such as this to be self-sustaining; it is the difference between pressures at the base of recharging and discharging columns of crustal fluid that creates a "hydrothermal siphon" capable of operating at a crustal scale (e.g., Stein and Fisher, 2003; Fisher et al., 2003).

Regional site surveys in preparation for Expedition 301 focused on and near basement outcrops that could be fluid entry and exit points to and from the crust, allowing hydrothermal flows to bypass generally thick and impermeable sediments (Fisher et al., 2003; Hutnak et al., 2006; **Zühlsdorff et al.**). Thermal data suggest a significant component of south to north (ridge-parallel) fluid flow in basement at the eastern end of the Leg 168 transect, an interpretation consistent with geochemical studies (Walker et al., 2007; Wheat et al., 2000). Consideration of bathymetric, sediment thickness, and heat flow data near the western end of the Leg 168 transect suggests that there may be a component of north to south fluid flow in basement in this area as well (Hutnak et al., 2006).

Two sets of numerical studies were completed to assess the regional thermal and hydrologic state of the upper crust in the Expedition 301 area, and to help place survey and drilling results in context. One set of numerical models was crafted to estimate basement properties consistent with inferred patterns and rates of fluid circulation between recharge and discharge sites separated by 50 km (the approximate distance between Grizzly Bare and Baby Bare outcrops) (Fig. F1B). These models complemented analytical calculations based on the same system geometry that suggested basement permeability in excess of 10^{-12} m^2 was required to allow formation of a self-sustaining hydrothermal siphon (Fisher et al., 2003). Numerical results suggested that outcrop to outcrop circulation can be sustained when basement permeability is $\geq 10^{-12}$ m^2 (Hutnak et al., 2006). At lower permeabilities, too much energy is lost during lateral fluid transport for circulation to continue without forcing, given the limited driving pressure difference at the base of recharging and discharging fluid columns.

These numerical models also showed that fluid temperatures in upper basement are highly sensitive to modeled permeability, providing a critical constraint on regional basement properties (Fig. F2A). When crustal permeability is too high (10^{-10} to 10^{-9}), fluid circulation is so rapid that basement is chilled to temperatures below those seen regionally (modeled values of 20°–50°C). A good match is achieved to observed upper basement temperatures of 60°–65°C (Davis et al., 1992; Hutnak et al., 2006; Shipboard Scientific Party, 1997; also see the **"Site U1301"** chapter) when lateral basement permeability is 10^{-11} m^2. These models were run with a two-dimensional domain; fully three-dimensional models are likely to require somewhat higher basement permeability to sustain conditions consistent with observations.

Another set of regional thermal models was created to evaluate the significance of "background" heat flow around the Expedition 301 work area. These models were prompted by a key observation following numerous regional thermal studies: heat flow along a 100 km long swath of 3.4–3.6 Ma seafloor, extending from 50 km north to 50 km south of ODP Sites 1026 and 1027, is lower by 15%–20% than predicted by standard lithospheric conductive cooling models, even after correcting for rapid sedimenta-

tion rates during the Pleistocene (an additional 12%–18% correction) (Davis et al., 1999; Hutnak et al., 2006; **Zühlsdorff et al.**).

Three explanations for the observed seafloor heat flow in this area were considered initially: (1) lithospheric heat flow is regionally low by 15%–20% in comparison to predictions from global lithospheric cooling models, (2) large-scale advective heat loss presently affects a 100 km long swath of seafloor (or perhaps an even large region), or (3) there is bias in the distribution of heat flow measurements. The first explanation seems especially ad hoc and would require anomalous lithospheric temperatures and/or structure, neither of which has been inferred from earlier studies. The second explanation is inconsistent with the lack of a spatial trend in heat flow values ≥5 km from outcrops and buried basement highs. Where advection has been inferred to explain heat flow suppression on the order of 15%–20% in other locations, there is generally lower heat flow near areas of recharge (e.g., Langseth and Herman, 1981; Stein and Fisher, 2003). The low values adjacent to Grizzly Bare outcrop extend only a few kilometers from the outcrop, and background heat flow away from this feature is identical to that away from Baby Bare and other outcrops to the north (**Zühlsdorff et al.**). The third explanation (sampling bias) remains possible but seems unlikely given the number and spatial coverage of available data and the consistency of background measurements (Hutnak et al., 2006).

Modeling allowed a new hypothesis to be explored: that the Expedition 301 work area is currently undergoing "thermal rebound" following the cessation of a long period of regionally efficient, advective heat extraction from the crust. A coupled model of heat transport and sedimentation was developed to assess the timing of rebound following the cessation of hydrothermal cooling and to check the extent of heat flow suppression likely to result from rapid sedimentation (Hutnak and Fisher, 2007). Rapid sedimentation tends to lower measured seafloor heat flow values by cooling near-seafloor sediments. The new model was an extension of earlier sedimentation models used for this area (Davis et al., 1999; Wang and Davis, 1992). The new model allows simulation of multiple basement layers beneath accumulating sediments. Heat sinks can be distributed within these layers as a proxy for advective heat loss caused by hydrothermal circulation, with the efficiency of the heat sinks representing the extent of hydrothermal heat extraction. Heat sinks are deactivated (either abruptly or gradually) to replicate the end or reduction of hydrothermal heat extraction, and the basement aquifer and overlying sediments are allowed to recover (rebound) conductively as sedimentation continues. This approach differs from that used in earlier analytical studies that assessed hydrothermal rebound (e.g., Benfield, 1949; Hobart et al., 1985) because the finite thickness of the basement aquifer in the newer models acts as a heat capacitor and delays recovery to lithospheric conditions. The model also can incorporate the influence of local convection within basement before and after the cessation of advective heat loss by using a high Nusselt number approximation.

Application of this model to the Expedition 301 field area suggests that the region may still be recovering from an earlier period of relatively efficient advective heat extraction from basement prior to the most recent period of Pleistocene sedimentation (Fig. **F2B**). Sedimentation rates were on the order of 250–440 m/m.y. during the last 1 m.y. around Sites 1026, 1027, and U1301 (Shipboard Scientific Party, 1997). Basement relief and sediment thickness maps in this area show numerous locations where sediment thickness is presently ≤100 m (Hutnak et al., 2006; **Zühlsdorff et al.**). Many basement areas now covered by thin sediments would have been exposed at the seafloor prior to the last several hundred thousand years of sedimentation, and areas of current basement exposure (e.g., Baby Bare outcrop) would have been larger (Fig. **F1C**). Larger areas of basement exposure and the greater spatial distribution of these areas would have been conducive to more efficient regional advective heat loss, as is currently seen at the western end of the Leg 168 transect (Davis et al., 1992; Hutnak et al., 2006), where measured heat flow is ~20% of lithospheric predictions, and on other ridge flanks where basement outcrops are more common (e.g., Hutnak et al., 2008; Lucazeau et al., 2006; Villinger et al., 2002).

We do not know the detailed history of hydrothermal heat extraction around the Expedition 301 field area during the Pleistocene, but we can assess the relative timing and magnitude of rebound following a reduction in advective heat loss (Fig. **F2**). If the efficiency of advective heat loss was initially 80%, as currently observed at the western end of the Leg 168 transect, then the abrupt cessation of advective heat loss in the last several hundred thousand years could result in regional heat flow at the seafloor being lower than the present lithospheric value by 15%–40% (taking into account the sedimentation history of this area, which should have lowered seafloor heat flow by 12%–18%). Assuming a lower initial efficiency for advective heat extraction would reduce the magnitude of remaining rebound, but if the advective extraction of lithospheric heat were reduced gradually as basement outcrops were buried (instead

of ending abruptly), then rebound would be delayed even more (Hutnak and Fisher, 2007).

This explanation for suppressed regional heat flow around the Expedition 301 field area would mean that the thermal and hydrogeologic state of the crust is recovering slowly from an earlier period of more vigorous low-temperature hydrothermal circulation. Thus upper basement temperatures around Sites 1026 and U1301, typically 60°–65°C, will continue to warm because of hydrothermal rebound and sedimentation, even while lithospheric heat flow becomes lower as the plate ages. This result implies that the decline in efficiency of regional advective heat extraction from the crust does not require a significant reduction in basement permeability. Instead, the reduction in the extent of closely spaced basement outcrops may be the primary explanation for anomalously warm basement conditions seen in this area at present, relative to similarly aged seafloor in other settings.

Expedition 301 drilling, coring, and logging

Site U1301 is 1 km south-southwest of Site 1026, where sediment thickness is 260–265 m above a buried basement high (Fig. **F1**). Hole U1301A was drilled without coring to 370 meters below seafloor (mbsf) (107 m subbasement [msb]). Casing was extended into the upper 15 m of basement, but poor hole conditions prevented installation of longer casing, coring, or deeper drilling. The large diameter and poor hole conditions also prevented geophysical logging in basement. Hole U1301B is 36 m away and penetrated to a total depth of 583 mbsf (318 msb). Uppermost basement was drilled without coring, and casing was installed to 85 msb. Basement was cored from 86 to 318 msb, with mean recovery of 30%, a value typical for upper basement rocks from young crust. The upper 100 m of the cored interval in Hole U1301B was irregular in diameter, often much larger than the maximum inflation diameter of packers to be used for hydrogeologic testing and CORK observatories. However, the lower 100 m of the hole was stable and to gauge, allowing collection of high-quality wireline logs and providing several horizons suitable for setting drill string and CORK casing packers. Relatively few basement holes have been drilled, cored, and logged to depths greater than 318 msb during four decades of scientific ocean drilling, and Hole U1301B penetrated younger seafloor than did other normal crustal holes of similar depth, so comparison with results from other sites is useful.

Basement rocks recovered from Hole U1301B consist mainly of aphyric to highly phyric pillow basalt, massive basalt, and basalt-hyaloclastite breccia, with pillow basalt being the most abundant (see the **"Site U1301"** chapter) (Fig. **F3**). The pillows have dominantly hypocrystalline textures with a glassy to microcrystalline groundmass and are sparsely to highly plagioclase ± clinopyroxene ± olivine phyric. Massive basalt consists of continuous sections comprising ≤4.5 m of similar lithology. The massive basalt is similar chemically to the sparsely phyric pillow basalt, and both have a bulk chemistry typical of normal mid-ocean-ridge basalt. They are sparsely to highly vesicular, with an average of 1%–5% round gas vesicles (up to 15% in some samples), ≤3 mm in diameter. Basalt-hyaloclastite breccia is represented by five core samples. Basement rocks are mostly slightly to moderately altered with secondary minerals that fill or line vesicles, fractures, veins, or cavities. Additional alteration minerals replace phenocrysts or replace interstitial mesostasis and glass. Alteration varies between 5% and 25% in massive and pillow basalts and is as high as 60% in basalt-hyaloclastite breccia. Principal secondary minerals are saponite, celadonite, and iron-oxyhydroxide, with minor carbonate, pyrite, and zeolite (see the **"Site U1301"** chapter).

Wireline logs collected from Hole U1301B included conventional caliper, natural gamma ray, bulk density, porosity, resistivity, and *P*-wave velocity tool runs. Logging data help to define the lithostratigraphy of Hole U1301B and establish whether or not conditions are as expected, in comparison to measurements made on core samples and borehole and core data collected from other basement holes (Bartetzko and Fisher, 2008; Tsuji and Iturrino, 2008). Logging data show that upper basement around Hole U1301B is highly layered at a scale of meters to tens of meters, similar to what is observed in other ocean crustal holes (e.g., Bartetzko et al., 2001; Jarrard et al., 2003; Pezard et al., 1992). Rapid penetration during drilling and poor hole conditions during casing operations suggest that the upper 85 m of basement is highly brecciated and poorly cemented. Irregular hole conditions continue to ~470 mbsf (~200 msb), below which the borehole diameter is consistent with the drill bit diameter. Wireline measurements of bulk density, *P*-wave velocity, and resistivity tend to be less than or equal to values determined from Hole U1301B core samples (Bartetzko and Fisher, 2008).

A comparison of wireline data from a global compilation of crustal holes shows that bulk density, *P*-wave velocity, and electrical resistivity tend to in-

crease with age, whereas core data decrease in bulk density and *P*-wave velocity with age (there are insufficient resistivity data from core samples for a meaningful evaluation of global age trends) (Bartetzko and Fisher, 2008). These changes in physical properties with crustal age are thought to result mainly from water-rock interaction during off-axis hydrothermal circulation. Circulating fluid seals voids and cracks with secondary minerals, leading to an increase in *P*-wave velocity, bulk density, and electrical resistivity at a large scale due to the decrease in porosity. Bulk density and *P*-wave velocity decrease at the scale of core samples because basalt alteration increases intergranular porosity and replacement of the original mineralogy by secondary minerals.

However, Hole U1301B bulk density and *P*-wave velocity core data fall below global trends—it is as if core samples from Hole U1301B came from much older seafloor, closer to 100 Ma based on measured values (Bartetzko and Fisher, 2008). Basaltic grain densities are also low, and formation factor values (an indication of pore tortuosity) are high. These anomalous core-scale physical properties may result from the particular hydrogeologic (and resulting thermal and chemical) history of Site U1301. Site U1301 is on a local buried basement high that was likely exposed at the seafloor and/or extensively cooled by rapidly flowing hydrothermal fluid until the late Pleistocene (Hutnak and Fisher, 2007). Until this time, the rate and extent of basement alteration would have been limited. A more recent phase of higher temperature fluid circulation with more restricted and less oxidative conditions followed after sediment buried nearby basement outcrops and greatly slowed the rate of fluid exchange between the crust and ocean. Anomalous core-scale properties may indicate stronger alteration and more enhanced replacement of original minerals by secondary phases at a microscale during the most recent period of alteration. In contrast, macroscale properties are more consistent with the preceding long period of low-temperature circulation.

CORK installations

Borehole observatories installed during Expedition 301 were designed to seal open holes so that thermal, pressure, and chemical conditions could equilibrate following the dissipation of the drilling disturbance; to facilitate collection of fluid and microbiological samples and temperature and pressure data using autonomous samplers and data logging systems; and to serve as long-term monitoring points for large-scale crustal testing. New observatory systems were designed to include a seafloor reentry cone and casing hanger(s); four concentric (nested) casing strings that penetrate through sediments and allow access to underlying basement; a series of seals (both between casing strings and between casing and the formation) that hydraulically isolate the open crustal interval at depth from the overlying ocean; downhole and seafloor instrumentation for collection of samples and data; and a seafloor wellhead that includes valves, fittings, electrical connections, and a landing platform so that the observatory can be serviced by submersible or ROV, allowing samples and data to be retrieved without recovery of the complete observatory assembly (**Fisher et al.**).

Hole 1026B was drilled to 295 mbsf, cased across the sediment/basement interface, and extended to 48 msb during Leg 168 (Shipboard Scientific Party, 1997). The original CORK installed in Hole 1026B included a data logger, pressure sensors, thermistors at multiple depths, and a fluid sampler, all of which were recovered in 1999 (except for the fluid sampler, which fell deeper into the hole). The original Hole 1026B CORK never completely sealed after being installed in 1996, and because crustal fluids are overpressured with respect to ambient hydrostatic conditions at Site 1026 (e.g., Davis et al., 1997; Davis and Becker, 2002; Fisher et al., 1997), this hole discharged fluid for years until the CORK was replaced during Expedition 301. As of the start of Expedition 301, warm (~64°C) altered basement fluid vented freely through the top of the wellhead.

Both of the Site U1301 boreholes contained four nested casing strings: 0.50 m (diameter) casing in the uppermost sediments, 0.41 m casing extending just across the sediment/basement interface, 0.27 m casing extending into basement, and 0.11 m inner CORK casing that houses instrument strings and plugs (Fig. **F3**). The two largest casing strings were sealed by collapse of unconsolidated sediments, and the 0.41 m string was also cemented across the sediment/basement interface. The annulus between 0.41 and 0.27 m casing strings at Site U1301 was supposed to contain a rubber mechanical casing seal near the seafloor, but this component was unfortunately not available for use during Expedition 301. An attempt was made to seal the 0.27 m casing strings at depth with cement, but rubbly basement prevented this cement from sealing between casing and the borehole wall. Operations were additionally complicated in Hole U1301B by the separation of the

unwelded 0.27 m casing string into two sections, leaving a gap just above the sediment/basement interface (Fig. **F3B**).

The CORK installed in Hole U1301A included a casing packer (as part of the 0.11 m inner casing) that was set inside 0.27 m casing. In contrast, the CORK installed in Hole U1301B included two casing packers set in open hole, intended to hydraulically isolate sections of the upper crust (**Fisher et al.;** also see the **"Site U1301"** chapter).

Hole 1027C was drilled during Leg 168, 2200 m east of Hole 1026C, where sediment thickness is 575 m above a buried basement low (Figs. **F1B, F3**). Hole 1027C penetrated to 632 mbsf. The upper part of the hole was cased through sediments and uppermost basement, with 54 m of open hole. The open interval near the base of Hole 1027C comprises a diabase sill, intercalated sediments, and basalt breccia overlying 26 m of extrusive volcanic rocks (Shipboard Scientific Party, 1997). A CORK installed in Hole 1027C during Leg 168 included a data logger, pressure sensors, thermistors at multiple depths, and a fluid sampler. These instruments were retrieved in 1999 to allow recovery of a basement fluid sampler, and the pressure logging system was replaced. In contrast to Hole 1026B, Hole 1027C was underpressured with respect to ambient hydrostatic conditions (–26 kPa) (Davis and Becker, 2002). Researchers intended to replace the CORK system in Hole 1027C during Expedition 301 but ran out of time and supplies. Thus the CORK in Hole 1027C remained fully sealed and recorded formation pressure before, during, and after Expedition 301.

Expedition 301 CORKs and the preexisting CORK in Hole 1027C were visited with the ROV *ROPOS* soon after the drilling expedition in September 2004 and again in September 2005 with the submersible *Alvin.* Data recovered during these dives showed that the Hole 1026B observatory was sealed and operating as intended, although the pressure in Hole 1026B was recovering slowly from the thermal perturbation associated with 8 y of upflow of warm formation fluid from the unsealed hole. CORKs in Holes U1301A and U1301B were incompletely sealed, for reasons discussed earlier, allowing cold ocean-bottom water to flow into the formation following CORK installation. The flow of cold water into the crust at Site U1301 caused a measurable pressure perturbation at Site 1027, 2.4 km away, comprising an inadvertent crosshole test.

Hydrogeologic experiments

Single- and crosshole pressure responses were interpreted from data collected during and after Expedition 301 to resolve hydrogeologic properties in the crust (Becker and Fisher, 2008; Fisher et al., 2008). Interpretation of single-hole tests is based on fitting pressure-time observations to an equation of the form

$$\Delta P = f(Q,t,T),$$

where Q is fluid pumping rate, t is time, and T is formation transmissivity. Transmissivity is the product of aquifer thickness and hydraulic conductivity, K, within a horizontal, tabular aquifer, where the latter is related to permeability by

$$k = K\mu/\rho g,$$

where μ is the viscosity and ρg is the specific weight of the fluid. Two independent variables are added in the case of a borehole pressure response during a crosshole test:

$$\Delta P = f(Q,t,T,r,S),$$

where r is the radial distance between perturbation and observation wells (known), and storativity, S, is

$$S = \rho g b(\alpha + n\beta),$$

where α is aquifer compressibility, n is porosity, and β is fluid compressibility. Thus, results from crosshole tests theoretically provide more information, but interpretation of these tests is also subject to additional assumptions (Becker and Fisher, 2008; Fisher et al., 2008).

If there is sufficient understanding of aquifer geometry and properties, one can account for deviations from ideal conditions such as heterogeneity and anisotropy (vertical and/or azimuthal), near-borehole damage resulting from drilling, leakage through overlying and/or underlying confining layers, and partial penetration of the well into the aquifer. Transmissivity and permeability are heterogeneous tensor quantities (particularly within fractured rocks), having values that vary with the temporal and spatial scales of testing. Formation storativity is a bulk (volumetric) scalar quantity, but it too can vary considerably with location, the spatial scale of testing, and the frequency of pressure perturbations. The different scales inherent in short-term (≤60 min) single-hole testing and longer term (13 month) crosshole testing provide some insight with regard to property scaling, but as discussed later, there may be influences of heterogeneity and anisotropy on different test responses as well.

Packer experiments during Expedition 301 were conducted with the same system and methods used dur-

ing Leg 168 and numerous earlier drilling expeditions (e.g., Becker and Fisher, 2000). The packer is made up as part of specialized bottom-hole assembly, lowered into a borehole to the desired depth, and inflated within casing or in the open formation (hole conditions permitting). A "go-devil" is dropped down the pipe to enable packer inflation. This device also carries autonomous pressure gauges that monitor conditions beneath the packer during pumping experiments. Digital gauges used during Expedition 301 were serviced and recalibrated prior to sailing and recorded pressures and temperatures throughout the experiments. Packer experiments such as these are limited in several ways. It is not possible to use pressure data from a pumping well to determine formation storage properties. In addition, the short testing time (≤60 min) results in estimates of formation transmissivity in the region immediately surrounding the borehole. One advantage of this latter restriction is that testing of multiple depth intervals during packer experiments provides insight to the layering of crustal hydrologic properties, at least close to the borehole.

Packer tests were attempted in Hole U1301A during Expedition 301, but the packer had to be set in 0.27 m casing above the open hole because the hole was oversized and in danger of collapsing (see the **"Site U1301"** chapter). Because the 0.27 m casing was not sealed at the base or inside the 0.41 m casing, these tests provide no useful information. In contrast, packer tests were run in Hole U1301B with the packer inflated in open hole, allowing determination of formation properties below the packer element. Only packer tests in Hole U1301B were interpreted (Becker and Fisher, 2008).

Packer setting depths in Hole U1301B were selected where basement rocks were relatively massive and the hole diameter was sufficiently small for the packer element to seal the hole and hold the packer in place, at 472, 442, and 417 mbsf (207, 177, and 152 msb, respectively) (Figs. **F3A, F4**). The deepest packer setting depth corresponds to an abrupt change in the character of basement geophysical logs. Above 470 mbsf (205 msb) the borehole diameter is highly irregular and there are intervals 10–50 m thick having very low bulk density, electrical resistivity, and *P*-wave velocity (Bartetzko and Fisher, 2008). Below ~470 mbsf (~200 msb), the borehole diameter is more consistent with the drill bit diameter, and zones of low bulk density are thinner and more widely spaced (Fig. **F3A**). This change in geophysical properties within the uppermost extrusive crust is similar to changes seen in other upper crustal sections (e.g., Bartetzko et al., 2001; Jarrard et al., 2003; Pezard et al., 1992).

Packer test records required several processing steps prior to interpretation, including corrections for superimposed perturbations related to tides, barometric pressure changes, and differences in fluid temperatures (Becker and Fisher, 2008). Examples of pressure-time records and interpretations from packer tests show typical formation and instrument responses and model fits (Fig. **F4**). Pressure tends to rise rapidly for the first few minutes of a pumping test, and then to rise more slowly for the duration of the test. In general, data are well fit by a conventional aquifer model, including assumptions of isotropic and homogeneous conditions; horizontal, radial flow into the formation; and laminar flow conditions at the borehole wall and within the aquifer (i.e., Darcy's law applies). The good fit of the data to an idealized model does not prove that such a model applies, but it suggests that more complex models may be difficult to justify on the basis of observational data. The use of a simple model also allows comparison of Expedition 301 test results to results from earlier packer tests at other locations, based on similar assumptions.

The geometric mean of results from packer tests at 472 mbsf are $T = 0.0034$ m^2/s and $k = 1.7 \times 10^{-12}$ m^2 (standard deviation [sd] = 2.3×10^{-13} m^2), whereas geometric mean values for tests at 442 and 417 mbsf are about twice as great ($T = 0.0064$ m^2/s and $k = 3.2 \times 10^{-12}$ m^2 [sd = 5.1×10^{-13} m^2]). This suggests that permeability may be significantly greater above 472 mbsf (207 msb), consistent with observed changes in geophysical logs (Fig. **F3**). If the consistent properties determined during the final four tests (setting depths of 442 and 417 mbsf) apply to the uppermost 207 m of basement, the geometric mean permeability within this interval is $k = 5 \times 10^{-12}$ m^2. In fact, the consistency of properties determined with setting depths of 442 and 417 mbsf suggests that most of the formation transmissivity may be concentrated between these depths. If we assume that the transmissivity occurs within this 30 m interval, the bulk permeability is $k = 2 \times 10^{-11}$ m^2 (Becker and Fisher, 2008).

A larger scale assessment of basement hydrogeologic properties was made from the long-term pressure perturbation observed in Hole 1027B that resulted from leakage of cold bottom seawater into the crust at Site U1301 (Fisher et al., 2008). The raw Hole 1027C pressure record was corrected for the influence of tides and other local oceanographic pro-

cesses and instrument drift. The residual signal shows the clear influence of basement operations during Expedition 301 (Fig. F5). Basement operations in Hole U1301B caused the greatest pressure response in Hole 1027C, whereas operations in Holes U1301A and 1026B had little or no influence. The packer experiments in Hole U1301B caused the greatest immediate perturbation, despite modest pumping rates, because this was when pumped fluids were forced to enter basement, rather than being allowed to flow back up the borehole to the overlying ocean. These observations suggest that shallow basement surrounding Hole U1301A may be less well connected hydrologically to the uppermost oceanic crust at the base of Hole 1027C than is deeper basement in Hole U1301B. In addition, the rate of pressure rise following emplacement of the subseafloor observatory in Hole U1301B is less than the rate of pressure rise following packer experiments or associated with drilling, coring, and other upper basement operations. These observations and consideration of the pressure-time response associated with flow down Hole U1301B allowed the flow rate into Hole U1301B during the 13 months following Expedition 301 to be estimated as Q = 2–5 L/s (Fisher et al., 2008).

Given this information, the basement aquifer transmissivity around Hole U1301B is inferred to be 0.005 to 0.012 m^2/s, suggesting bulk permeability within the upper 300 m of crust of $k = 0.7 \times 10^{-12}$ m^2 to 2×10^{-12} m^2. These values correspond to basement aquifer storativity of $S = 1 \times 10^{-3}$ to 3×10^{-3}, which implies aquifer compressibility of $\alpha = 3 \times 10^{-10}$ Pa^{-1} to 9×10^{-10} Pa^{-1}, a value close to or somewhat larger than that of seawater. The transmissivity and permeability values are at the lower end of estimates based on single-hole packer experiments, even though they result from testing of a much larger rock volume, extending perhaps 10–30 km from the borehole (assuming isotropic and homogeneous conditions) (Fisher et al., 2008). In addition, basement hydrogeologic properties estimated from this crosshole response are 1 to 3 orders of magnitude lower than estimates based on numerical modeling and calculations based on tidal responses and drainage following tectonic strain events, which test similar crustal volumes (Fig. F6). One explanation for this difference in inferred properties is that properties in the crust around Site U1301 may be anisotropic.

Anisotropy in the seismic properties of oceanic basement rocks is thought to result from preferential orientation of cracks, faults, and fractures (i.e., the crustal "fabric") (e.g., Sohn et al., 1997; Stephen, 1981). The dominant crustal fabric is generally thought to be subparallel to the orientation of the mid-ocean ridge where the crust was created. This fabric may favor fluid flow in the crust in the "along-strike" direction (Delaney et al., 1992; Haymon et al., 1991; Wilcock and Fisher, 2004), an interpretation consistent with geochemical and thermal data from the Expedition 301 field area (Fisher et al., 2003; Hutnak et al., 2006; Walker et al., 2007; Wheat et al., 2000). Calculations show how azimuthal anisotropy could influence the permeability apparent from a crosshole experiment involving a single observation borehole (Fig. F5B). If the angle of measurement is oblique relative to the direction of greatest permeability, the measured value will be very close to that in the lowest permeability direction, even for a large anisotropy ratio.

Unfortunately, there are insufficient data in this area at present to quantify crustal permeability anisotropy, but such an assessment should be possible after the next drilling expedition, as discussed below. If the crust in this area is shown to be azimuthally anisotropic, this will require reinterpretation of data analyzed in many earlier studies that assumed primarily one-dimensional or two-dimensional (across-strike) geometries for fluid flow in basement.

Summary of hydrogeologic findings and plans for future work

Expedition 301 hydrogeologic test results stand out in comparison with the rest of the global data set of results from similar experiments (Fig. F6). The global data set tends to show a decrease in bulk permeability with depth into basement. Values higher than 10^{-13} m^2 are restricted to the upper 300 m of basement, although data from deeper crustal levels are limited. Tests of smaller depth intervals in upper basement tend to yield higher permeabilities, as often seen in field studies and data compilations from aquifers and crustal systems on land. Packer test results from Hole U1301B appear to be anomalously high in comparison to the global permeability versus depth trend based on packer and thermal flow meter experiments (Fig. F6) and permeability versus age trends for the upper basaltic crust (Becker and Davis, 2003; Fisher and Becker, 2000). Curiously, bulk permeabilities inferred from packer tests are at the limit of those inferred from regional hydrogeologic models (Hutnak et al., 2006). In other locations, packer experiments tend to yield bulk permeability values that are 0.5–1.0 orders of magnitude lower than those determined using a thermal flow meter in the same holes,

and both of these experimental methods tend to yield bulk permeability values 2–4 orders of magnitude lower than those inferred from numerical modeling and analysis of responses to tidal pressure variations and tectonic events. This difference in calculated properties is generally attributed to the heterogeneous nature of permeability within the oceanic crust and the characteristic scales and assumptions inherent in the different methods.

It is curious that basement permeability estimates made from the crosshole response between Sites U1301 and 1027 are lower than estimates based on packer experiments in Hole U1301B, even through the latter experiment tested a much smaller volume of crustal rock. This could result from azimuthal anisotropy in basement permeability, as described earlier, or perhaps basement around Site U1301 is unusually permeable because it only recently ended a long phase of vigorous, low-temperature hydrothermal circulation that kept the crust cool and limited the extent of alteration (Hutnak and Fisher, 2007). Completion of the next drilling expedition and the subsequent crosshole testing program should help to resolve the extent of crustal heterogeneity and anisotropy in this area.

As of summer 2008, Holes U1301A and U1301B remain unsealed. Attempts to seal Hole U1301B using a cement delivery system with the submersible *Alvin* in summers 2006 and 2007 were unsuccessful. The U.S. IODP R/V *JOIDES Resolution* will return to Site U1301 in summer 2009 to conduct additional cementing operations, pumping much larger volumes than is possible using a submersible.

Shimmering fluid was observed discharging from Hole U1301A during and after summer 2007 dive operations. No such evidence for upflow from the borehole was observed during earlier visits, suggesting that Hole U1301A must have "turned around" sometime between 2006 and 2007 servicing operations. In fact, downhole temperature loggers recovered from Hole U1301A in summer 2008 provide a detailed record of this flow reversal, which appears to have occurred spontaneously when the formation overpressure recovered sufficiently so as to overcome the excess pressure generated by cold, downflowing fluids. Why this required 3 y following Expedition 301 is not understood. Remarkably, Hole U1301B continues to draw fluid rapidly into basement, even though it is located just 36 m from Hole U1301A, which is vigorously discharging warm formation fluid to the ocean. The turnaround of flow in Hole U1301A in 2007 has no influence on the interpretation of crosshole response between Holes U1310B and 1027C, based on data collected in 2004–2005 (Fisher et al., 2008). But understanding of the pressure and thermal interactions between Holes U1301A and U1301B and implications for local and regional crustal hydrogeology will require additional investigation.

The next drilling expedition to the Expedition 301 area appeared on the IODP 2008 schedule briefly in 2007, but then the expedition was postponed when the *JOIDES Resolution* went into dry-dock for refit. Expedition 301 proponents have an additional observatory servicing expedition with the *Alvin* scheduled for summer 2009, after the drillship cements the unsealed CORKs at Site U1301, but little more can be done to advance long-term experimental objectives until the next full drilling expedition.

The next drilling expedition will begin with operations in Hole 1027C, recovering the existing CORK and deepening the hole by 30–40 m. This will make room to hang drill collars (making CORK installation safer), provide upper-crustal samples for microbiological and other analyses, and open up the formation for large-scale testing. Emplacement of a two-level CORK system will optimize the configuration for crosshole tests and allow acquisition of long-term geochemical and microbiological samples.

Hole SR-2A (Fig. **F1C**) will be the deeper of two new basement holes, located between Sites 1026 and U1301. The operational approach in Hole SR-2A will be similar to that used for Hole U1301B on Expedition 301, with drilling, casing, coring, wireline logs, single-hole packer work, and emplacement of a multilevel CORK. Nearby Hole SR-2B will penetrate the upper, most permeable crustal layer(s) and will be the main perturbation well for long-term experiments. Once this hole is drilled and (partially) cased, researchers will initiate a 24 h pumping test with seawater and tracers, then set a multilevel CORK observatory. Multiyear crosshole tests will be run by submersible or ROV 1–2 y after drilling operations are complete, using the naturally overpressured formation and an autonomous flow meter to test properties within an enormous crustal volume surrounding the boreholes.

Work completed thus far shows that crosshole testing can be done at a crustal scale using CORK observatories. The development of tools and methods that allow this kind of testing comprises a significant accomplishment for the scientific ocean drilling community. Instruments and methods developed for Expedition 301 are now being adapted for use in other settings, and researchers are likely to see similarly

ambitious experimental programs undertaken around the world in coming decades. Long-term borehole observatories provide opportunities to explore the subseafloor realm in new ways, across a broader range of processes and scales, and with greater accuracy and resolution than was possible in the past. It is challenging to install, maintain, and use these systems, but persistence and patience is providing a new and more nuanced understanding of marine hydrogeologic systems.

Acknowledgments

This research used data provided by the Ocean Drilling Program (ODP) and the Integrated Ocean Drilling Program (IODP) and was supported by U.S. National Science Foundation grants OCE–0550713 and OCE–0727952 and Joint Oceanographic Institutions (JOI), Inc., Projects T301A7 and T301B7. Reviews by P. Flemings, H. Villinger, and A. Klaus improved this paper.

References

Bartetzko, A., and Fisher, A.T., 2008. Physical properties of young (3.5 Ma) oceanic crust from the eastern flank of the Juan de Fuca Ridge: comparison of wireline and core measurements with global data. *J. Geophys. Res., [Solid Earth],* 113(B5):B05105. **doi:10.1029/2007JB005268**

Bartetzko, A., Pezard, P., Goldberg, D., Sun, Y.-F., and Becker, K., 2001. Volcanic stratigraphy of DSDP/ODP Hole 395A: an interpretation using well-logging data. *Mar. Geophys. Res.,* 22(2):111–127. **doi:10.1023/A:1010359128574**

Becker, K., and Davis, E.E., 2003. New evidence for age variation and scale effects of permeabilities of young oceanic crust from borehole thermal and pressure measurements. *Earth Planet. Sci. Lett.,* 201(3–4):499–508. **doi:10.1016/S0012-821X(03)00160-2**

Becker, K., and Fisher, A.T., 2000. Permeability of upper oceanic basement on the eastern flank of the Juan de Fuca Ridge determined with drill-string packer experiments. *J. Geophys. Res.,* 105(B1):897–912. **doi:10.1029/1999JB900250**

Becker, K., and Fisher, A.T., 2008. Borehole packer tests at multiple depths resolve distinct hydrologic intervals in 3.5-Ma upper oceanic crust on the eastern flank of Juan de Fuca Ridge. *J. Geophys. Res., [Solid Earth],* 113(B7):B07105. **doi:10.1029/2007JB005446**

Benfield, A.E., 1949. The effect of uplift and denudation on underground temperatures. *J. Appl. Phys.*, 20(1):66–70. **doi:10.1063/1.1698238**

Bruns, T.R., and Lavoie, D.L., 1994. Bulk permeability of young backarc basalt in the Lau Basin from a downhole packer experiment (Hole 839B). *In* Hawkins, J., Parson, L., Allan, J., et al., *Proc. ODP, Sci. Results,* 135: College Station, TX (Ocean Drilling Program), 805–816. **doi:10.2973/odp.proc.sr.135.150.1994**

Davis, E.E., and Becker, K., 2002. Observations of natural-state fluid pressures and temperatures in young oceanic crust and inferences regarding hydrothermal circulation. *Earth. Planet. Sci. Lett.,* 204(1–2):231–248. **doi:10.1016/S0012-821X(02)00982-2**

Davis, E.E., Chapman, D.S., Mottl, M.J., Bentkowski, W.J., Dadey, K., Forster, C., Harris, R., Nagihara, S., Rohr, K., Wheat, G., and Whiticar, M., 1992. FlankFlux: an experiment to study the nature of hydrothermal circulation in young oceanic crust. *Can. J. Earth Sci.,* 29(5):925–952.

Davis, E.E., Chapman, D.S., Wang, K., Villinger, H., Fisher, A.T., Robinson, S.W., Grigel, J., Pribnow, D., Stein, J., and Becker, K., 1999. Regional heat flow variations across the sedimented Juan de Fuca Ridge eastern flank: constraints on lithospheric cooling and lateral hydrothermal heat transport. *J. Geophys. Res.,* 104(B8):17675–17688. **doi:10.1029/1999JB900124**

Davis, E.E., and Currie, R.G., 1993. Geophysical observations of the northern Juan de Fuca Ridge system: lessons in sea-floor spreading. *Can. J. Earth Sci.,* 30:278–300.

Davis, E.E., Fisher, A.T., Firth, J.V., et al., 1997. *Proc. ODP, Init. Repts.,* 168: College Station, TX (Ocean Drilling Program). **doi:10.2973/odp.proc.ir.168.1997**

Davis, E.E., Wang, K., He, J., Chapman, D.S., Villinger, H., and Rosenberger, A., 1997. An unequivocal case for high Nusselt number hydrothermal convection in sediment-buried igneous oceanic crust. *Earth Planet. Sci. Lett.,* 146(1–2):137–150. **doi:10.1016/S0012-821X(96)00212-9**

Delaney, J.R., Robigou, V., McDuff, R.E., and Tivey, M.K., 1992. Geology of a vigorous hydrothermal system on the Endeavour segment, Juan de Fuca Ridge. *J. Geophys. Res., [Solid Earth],* 97(B13):19663–19682. **doi:10.1029/92JB00174**

Elderfield, H., Wheat, C.G., Mottl, M.J., Monnin, C., and Spiro, B., 1999. Fluid and geochemical transport through oceanic crust: a transect across the eastern flank of the Juan de Fuca Ridge. *Earth Planet. Sci. Lett.,* 172(1–2):151–165. **doi:10.1016/S0012-821X(99)00191-0**

Engelen, B., Ziegelmüller, K., Wolf, L., Köpke, B., Gittel, A., Cypionka, H., Treude, T., Nakagawa, S., Inagaki, F., Lever, M.A., and Steinsbu, B.O., 2008. Fluids from the ocean crust support microbial activities within the deep biosphere. *Geomicrobiol. J.,* 25(1):56–66. **doi:10.1080/01490450701829006**

Fisher, A.T., and Becker, K., 2000. Channelized fluid flow in oceanic crust reconciles heat-flow and permeability data. *Nature (London, U. K.),* 403(6765):71–74. **doi:10.1038/47463**

Fisher, A.T., Becker, K., and Davis, E.E., 1997. The permeability of young oceanic crust east of Juan de Fuca Ridge determined using borehole thermal measurements. *Geophys. Res. Lett.,* 24(11):1311–1314. **doi:10.1029/97GL01286**

Fisher, A.T., Davis, E.E., and Becker, K., 2008. Borehole-to-borehole hydrologic response across 2.4 km in the upper oceanic crust: implications for crustal-scale properties. *J. Geophys. Res.*, 113(B7):B07106. **doi:10.1029/2007JB005447**

Fisher, A.T., Davis, E.E., Hutnak, M., Spiess, V., Zühlsdorff, L., Cherkaoui, A., Christiansen, L., Edwards, K., Macdonald, R., Villinger, H., Mottl, M.J., Wheat, C.G., and Becker, K., 2003. Hydrothermal recharge and discharge across 50 km guided by seamounts on a young ridge flank. *Nature (London, U. K.),* 421(6923):618–621. **doi:10.1038/nature01352**

Goto, S., and Matsubayashi, O., 2008. Inversion of needle-probe data for sediment thermal properties of the eastern flank of the Juan de Fuca Ridge. *J. Geophys. Res.*, 113(B8):B08105. **doi:10.1029/2007JB005119**

Haymon, R.M., Fornari, D.J., Edwards, M.H., Carbotte, S., Wright, D., and Macdonald, K.C., 1991. Hydrothermal vent distribution along the East Pacific Rise crest (9°09′–54′N) and its relationship to magmatic and tectonic processes on fast-spreading mid-ocean ridges. *Earth Planet. Sci. Lett.,* 104(2–4):513–534. **doi:10.1016/0012-821X(91)90226-8**

Heuer, V., Elvert, M., Tille, S., Krummen, M., Prieto Mollar, X., Hmelo, L.R., and Hinrichs, K.-U., 2006. Online $\delta^{13}C$ analysis of volatile fatty acids in sediment/porewater systems by liquid chromatography-isotope ratio mass spectrometry. *Limnol. Oceanogr.: Methods,* 4:346–357.

Hobart, M.A., Langseth, M.G., and Anderson, R.N., 1985. A geothermal and geophysical survey on the south flank of the Costa Rica Rift: Sites 504 and 505. *In* Anderson, R.N., Honnorez, J., Becker, K., et al., *Init. Repts. DSDP,* 83: Washington, DC (U.S. Govt. Printing Office), 379–404. **doi:10.2973/dsdp.proc.83.122.1985**

Hutnak, M., and Fisher, A.T., 2007. Influence of sedimentation, local and regional hydrothermal circulation, and thermal rebound on measurements of seafloor heat flux. *J. Geophys. Res., [Solid Earth],* 112(B12):B12101. **doi:10.1029/2007JB005022**

Hutnak, M., Fisher, A.T., Harris, R., Stein, C., Wang, K., Spinelli, G., Schindler, M., Villinger, H., and Silver, E., 2008. Large heat and fluid fluxes driven through mid-plate outcrops on ocean crust. *Nat. Geosci.,* 1(9):611–614. **doi:10.1038/ngeo264**

Hutnak, M., Fisher, A.T., Zühlsdorff, L., Spiess, V., Stauffer, P.H., and Gable, C.W., 2006. Hydrothermal recharge and discharge guided by basement outcrops on 0.7–3.6 Ma seafloor east of the Juan de Fuca Ridge: observations and numerical models. *Geochem., Geophys., Geosyst.,* 7(7):Q07O02. **doi:10.1029/2006GC001242**

Jarrard, R.D., Abrams, L.J., Pockalny, R., Larson, R.L., and Hirono, T., 2003. Physical properties of upper oceanic crust: Ocean Drilling Program Hole 801C and the waning of hydrothermal circulation. *J. Geophys. Res., [Solid Earth],* 108(B4):2188. **doi:10.1029/2001JB001727**

Kiyoka, S., and Yokoyama, K., submitted. Provence of turbidite sands at IODP Expedition 301 in the northwestern Cascadia Basin, western North America. *Math. Geol.*

Langseth, M.G., and Herman, B.M., 1981. Heat transfer in the oceanic crust of the Brazil Basin. *J. Geophys. Res., [Solid Earth],* 86(B11):10805–10819. **doi:10.1029/JB086iB11p10805**

Lever, M.A., Alperin, M., Engelen, B., Inagaki, F., Nakagawa, S., Steinsbu, B.O., Teske, A., and IODP Expedition Scientists, 2006. Trends in basalt and sediment core contamination during IODP Expedition 301. *Geomicrobiol. J.,* 23(7):517–530. **doi:10.1080/01490450600897245**

Lipp, J.S., Morono, Y., Inagaki, F., and Hinrichs K.-U., 2008. Significant contribution of Archaea to extant biomass in marine subsurface sediments. *Nature (London, U. K.),* 454(7207):991–994. **doi:10.1038/nature07174**

Lucazeau, F., Bonneville, A., Escartin, J., Von Herzen, R.P., Gouze, P., Carton, H., Cannat, M., Vidal, V., and Adam, C., 2006. Heat flow variations on a slowly accreting ridge: constraints on the hydrothermal and conductive cooling for the Lucky Strike segment (Mid-Atlantic Ridge, 37°N), *Geochem., Geophys., Geosyst.,* 7(7):Q07011. **doi:10.1029/2005GC001178**

Nakagawa, S., Inagaki, F., Suzuki, Y., Steinsbu, B.O., Lever, M.A., Takai, K., Engelen, B., Sako, Y., Wheat, C.G., Horikoshi, K., and Integrated Ocean Drilling Program Expedition 301 Scientists, 2006. Microbial community in black rust exposed to hot ridge-flank crustal fluids. *Appl. Environ. Microbiol.,* 72(10):6789–6799. **doi:10.1128/AEM.01238-06**

Pezard, P.A., Anderson, R.N., Ryan, W.B.F., Becker, K., Alt, J.C., and Gente, P., 1992. Accretion, structure and hydrology of intermediate spreading-rate oceanic crust from drillhole experiments and seafloor observations. *Mar. Geophys. Res.*, 14(2):93–123. **doi:10.1007/BF01204282**

Rosenberger, A., Davis, E.E., and Villinger, H., 2000. Data report: hydrocell-95 and -96 single-channel seismic data on the eastern Juan de Fuca Ridge flank. *In* Fisher, A., Davis, E.E., and Escutia, C. (Eds.), *Proc. ODP, Sci. Results,* 168: College Station, TX (Ocean Drilling Program), 9–19. **doi:10.2973/odp.proc.sr.168.021.2000**

Shipboard Scientific Party, 1997. Rough basement transect (Sites 1026 and 1027). *In* Davis, E.E., Fisher, A.T., Firth, J.V., et al., *Proc. ODP, Init. Repts.,* 168: College Station, TX (Ocean Drilling Program), 101–160. **doi:10.2973/odp.proc.ir.168.105.1997**

Sohn, R.A., Webb, S.C., Hildebrand, J.A., and Cornuelle, B.D., 1997. Three-dimensional tomographic velocity structure of upper crust, CoAxial segment, Juan de Fuca Ridge: implications for on-axis evolution and hydrothermal circulation. *J. Geophys. Res.*, 102(B8):17679–17695. **doi:10.1029/97JB00592**

Stein, J.S., and Fisher, A.T., 2003. Observations and models of lateral hydrothermal circulation on a young ridge flank: numerical evaluation of thermal and chemical constraints. *Geochem., Geophys., Geosyst.,* 4(3):1026. **doi:10.1029/2002GC000415**

Stephen, R.A., 1981. Seismic anisotropy observed in upper oceanic crust. *Geophys. Res. Lett.,* 8(8):865–868. **doi:10.1029/GL008i008p00865**

Tsuji, T., and Iturrino, G.J., 2008. Velocity-porosity relationships in oceanic basalt from eastern flank of the Juan de Fuca Ridge: the effect of crack closure on seismic velocity. *Explor. Geophys.,* 39(1):41–51. **doi:10.1071/EG08001**

Villinger, H., Grevemeyer, I., Kaul, N., Hauschild, J., and Pfender, M., 2002. Hydrothermal heat flux through aged oceanic

crust: where does the heat escape? *Earth Planet. Sci. Lett.*, 202(1):159–170. **doi:10.1016/S0012-821X(02)00759-8**

Walker, B.D., McCarthy, M.D., Fisher, A.T., and Guilderson, T.P., 2007. Dissolved inorganic carbon isotopic composition of low-temperature axial and ridge-flank hydrothermal fluids of the Juan de Fuca Ridge. *Mar. Chem.*, 108(1–2):123–136. **doi:10.1016/j.marchem.2007.11.002**

Wang, K., and Davis, E.E., 1992. Thermal effects of marine sedimentation in hydrothermally active areas. *Geophys. J. Int.*, 110(1):70–78. **doi:10.1111/j.1365-246X.1992.tb00714.x**

Wheat, C.G., Elderfield, H., Mottl, M.J., and Monnin, C., 2000. Chemical composition of basement fluids within an oceanic ridge flank: implications for along-strike and across-strike hydrothermal circulation. *J. Geophys. Res.*, 105(B6):13437–13447. **doi:10.1029/2000JB900070**

Wheat, C.G., and McManus, J., 2008. Germanium in mid-ocean ridge flank hydrothermal fluids. *Geochem., Geophys., Geosyst.*, 9(3):Q03025. **doi:10.1029/2007GC001892**

Wilcock, W.S.D., and Fisher, A.T., 2004. Geophysical constraints on the subseafloor environment near mid-ocean ridges. *In* Cary, C., et al. (Eds.), *Subseafloor Biosphere at Mid-Ocean Ridges:* Washington, DC (Am. Geophys. Union), 51–74.

Initial receipt: 9 September 2008
Acceptance: 1 March 2009
Publication: 13 May 2009
MS 301-206

Figure F1. Expedition 301 field area. **A.** Index map of ODP Leg 168 drilling transect (thick black line), Expedition 301 work area (gold star), Juan de Fuca Ridge, and nearby continental areas. Inset profile of Leg 168 sites mentioned in the text. **B.** Regional bathymetric map of Holes 1026B and 1027C and Site U1301. **C.** Basement relief from bathymetric and seismic data with ODP and IODP drill sites. White areas = present-day basement outcrops. Figure modified from **Zühlsdorff et al.**

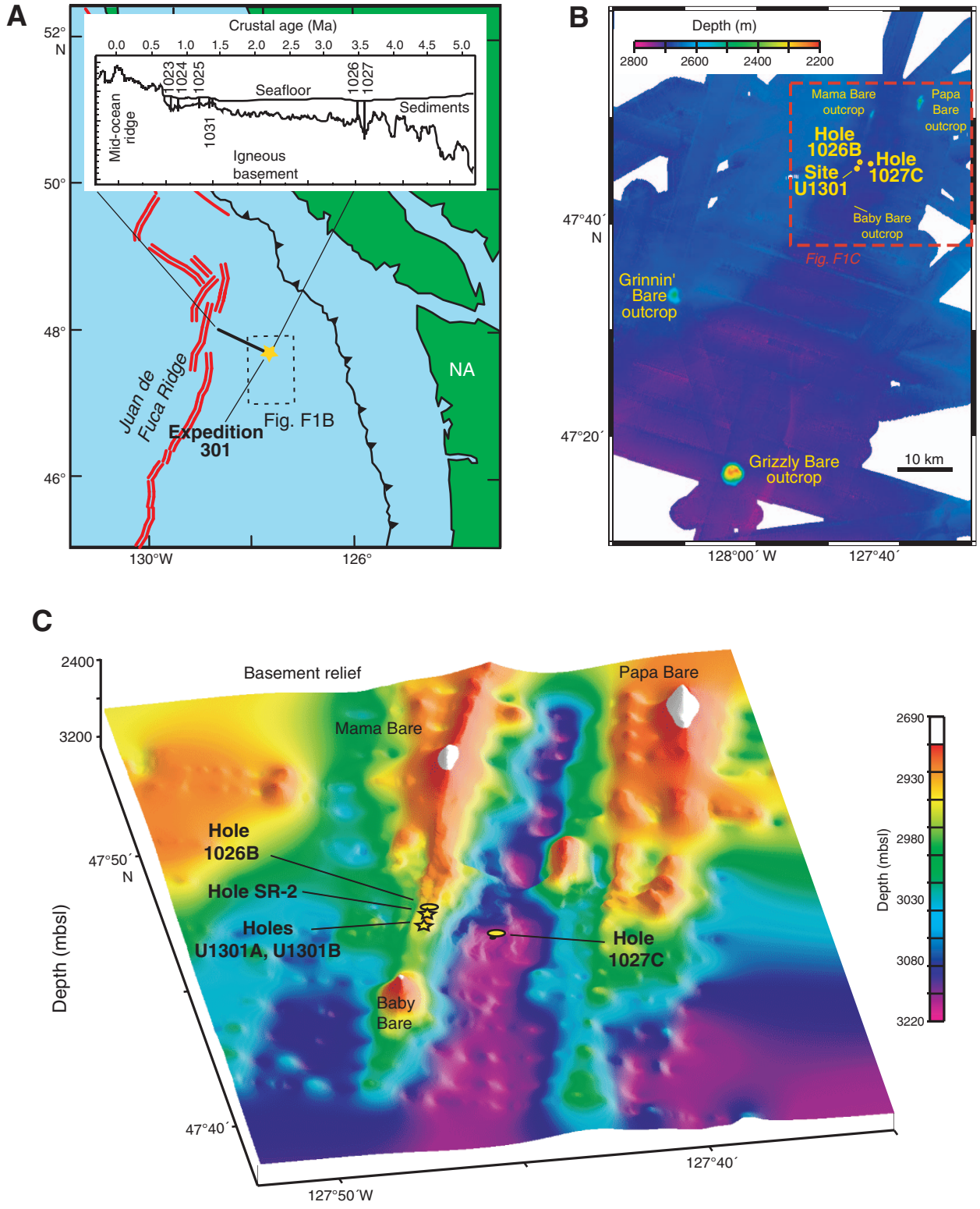

Figure F2. Selected results of thermal and fluid flow models in the Expedition 301 field area. **A.** Basement recharge and discharge temperatures from transient, two-dimensional, self-sustaining, outcrop to outcrop models of coupled fluid and heat flow (Hutnak et al., 2006). Blue = temperatures within recharge areas, red = temperatures within discharge areas. Curves extend to different depths depending on the thickness of the basement aquifer. Vertical band = observed and inferred regional basement temperature range (60°–65°C) consistent with the chemistry of upper crustal fluids. Modeled upper basement temperatures are excessively cooled when basement permeability exceeds 10^{-11} m^2. Permeability ≤10^{-12} m^2 allows basement to become too warm, and eventually prevents formation of a hydrothermal siphon. Three-dimensional simulations would likely shift these curves somewhat to the right (Hutnak et al., 2006). **B.** Calculated seafloor heat flow fraction vs. time for ODP Sites 1026 (thick curves) and 1027 (thin curves), assuming an initial 80% efficiency in regional advective extraction of lithospheric heat by hydrothermal circulation, followed by cessation at 0.5 (solid lines), 0.2 (dashed lines), and 0.1 Ma (dotted lines) (modified from Hutnak and Fisher, 2007). Stippled band = magnitude of likely sedimentation corrections appropriate for these sites based on the known sedimentation history. Striped box = mean and ±1 standard deviation (sd) of filtered seafloor heat flow observations from 3.4 to 3.6 Ma seafloor extending 50 km north and south of the Expedition 301 field area (Hutnak et al., 2006).

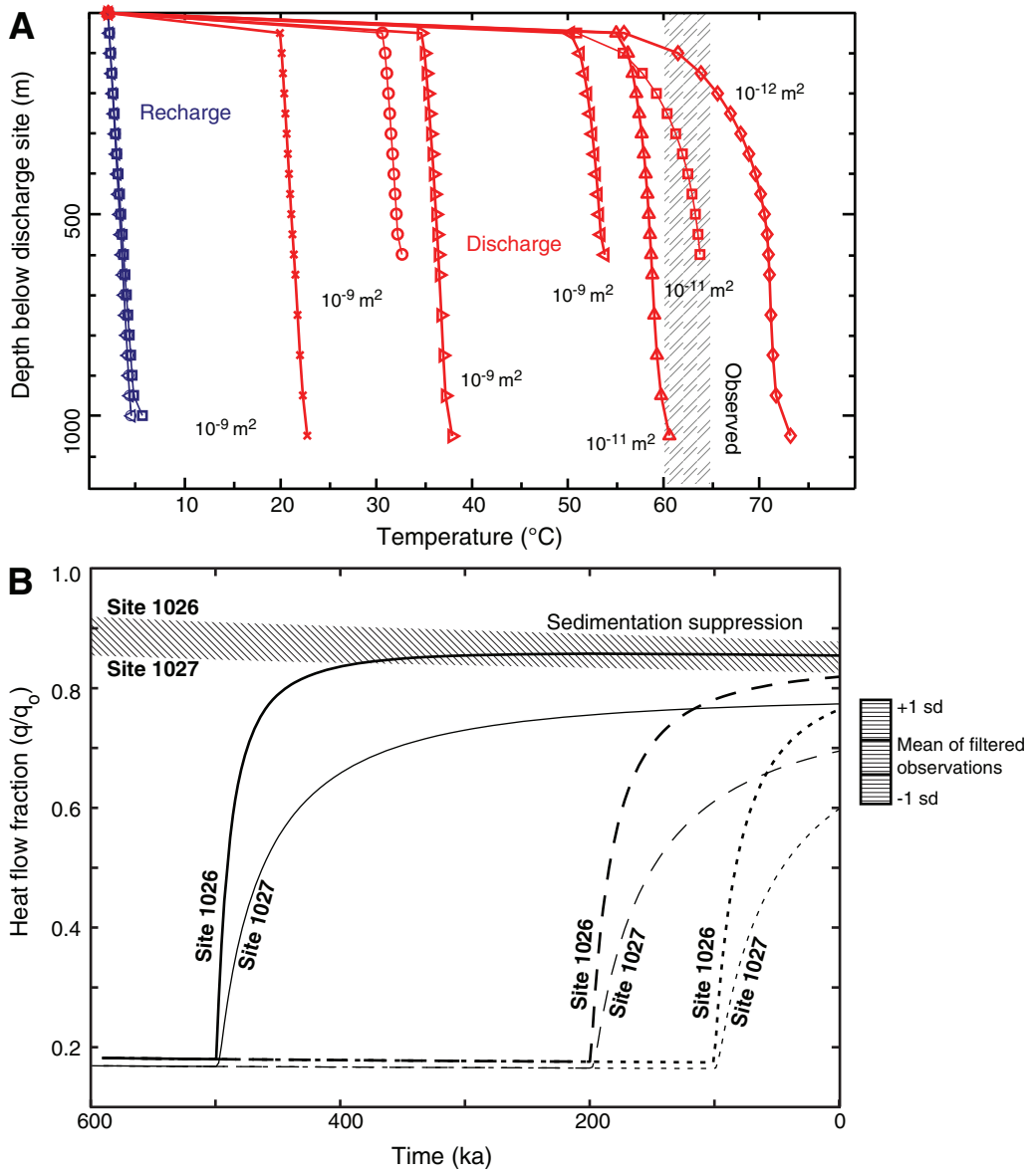

Figure F3. Summary of basement and borehole observatory characteristics, Holes 1027C and U1301B (modified from Fisher et al., 2008). **A.** Basement recovery, primary lithology, borehole size, and bulk density, Hole U1301B (see the **"Expedition 301 summary"** chapter). Basement cores were collected from ~355 to 575 mbsf (~100 to 320 msb), with recovery indicated by black intervals next to depth column. Borehole diameter was measured with wireline caliper tool. Note large washed-out intervals above 470 mbsf (220 msb). Bulk density log (line) and analyses of pieces of rock (diamonds) show evidence for considerable porosity in uppermost basement and a layered basement structure especially below 470 mbsf (220 msb), with alternating more and less dense intervals. Horizontal bands = depths where CORK casing packers and the drill string packer used for hydrogeologic testing were set against the borehole wall. **B.** Casing and CORK configurations, Holes U1301B and 1027C. TD = total depth.

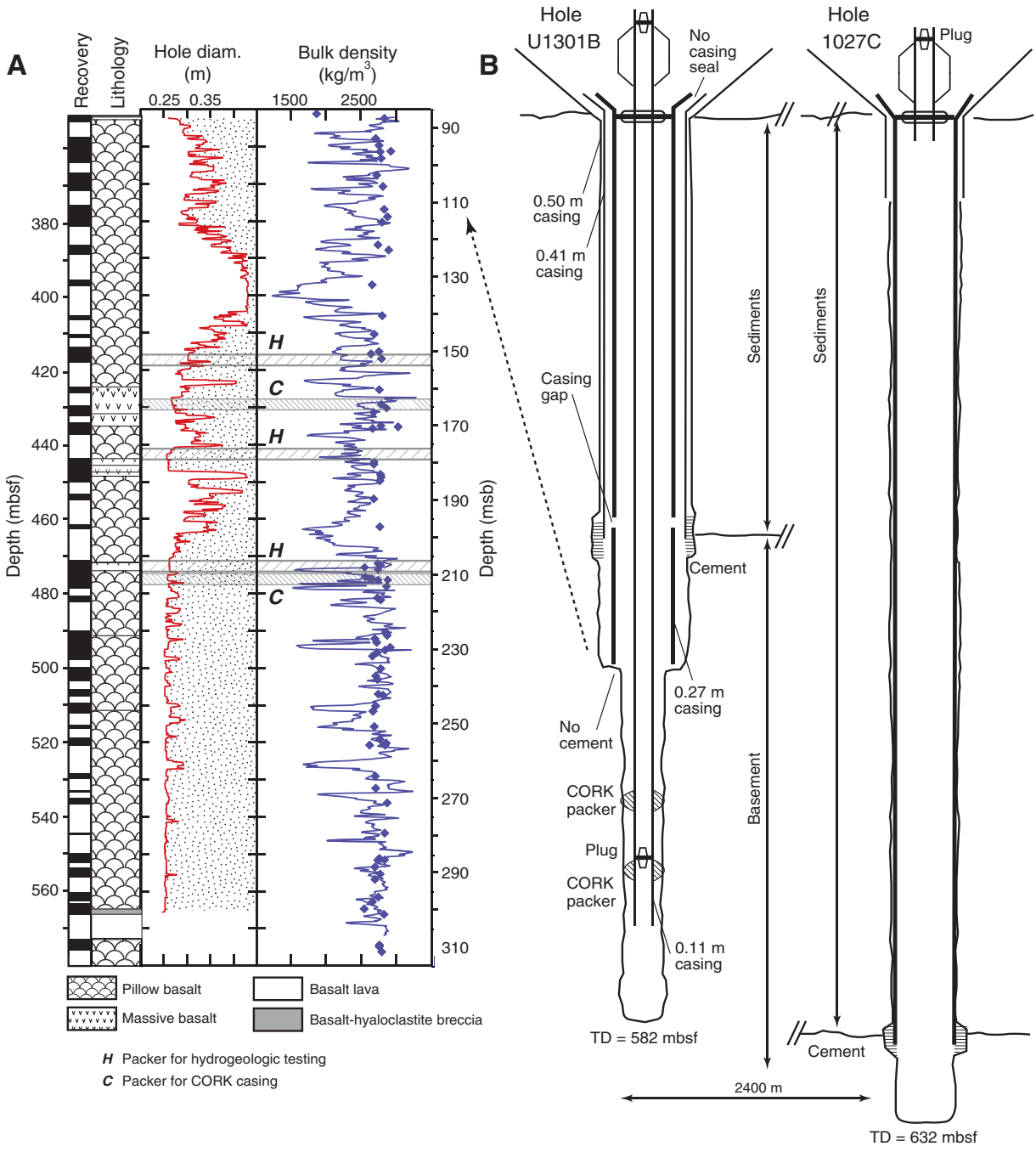

Figure F4. Downhole gauge pressure (solid line) and temperature (dashed line) record during packer experiments, Hole U1301B (modified from Becker and Fisher, 2008). At the first setting depth of 472 mbsf, cold hydrostatic pressure in the hole was monitored for 30 min (H) before actual packer inflation (I). At each inflation depth, packer inflation produces an uncontrolled pulse in the pressure record as a sliding sleeve is shifted to lock the packers inflated and open a passageway from the pressurized drill string to the formation isolated below the packer element (S). Inset plots show example fits of analytical radial flow model to filtered packer pressure records, with time relative to the start of individual injection tests.

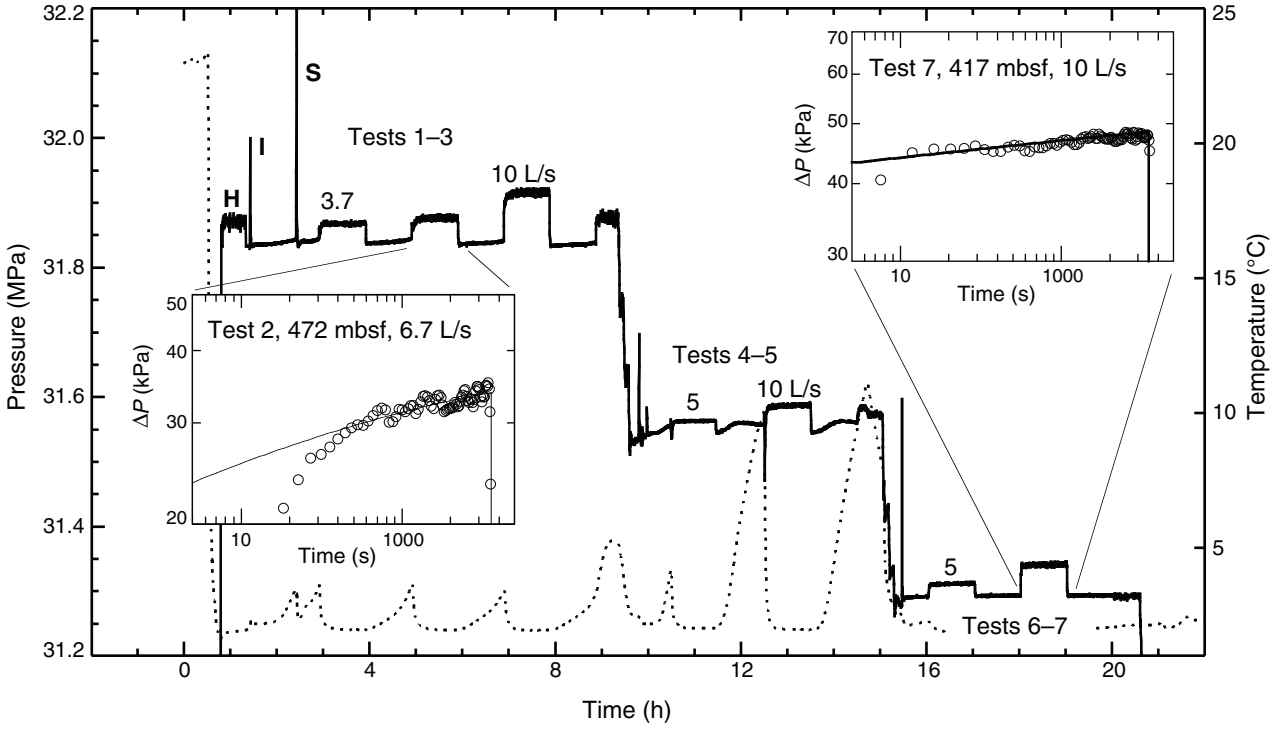

Figure F5. Observations and calculations from crosshole test. **A.** Filtered pressure time record from Hole 1027C, beginning 6 months before and ending 13 months after Expedition 301 (modified from Fisher et al., 2008). Striped vertical band = period of basement drilling, coring, casing, and testing operations during Expedition 301. Smooth curve shows least-squares best fit of observations to analytical calculations for the pressure response in Hole 1027C to flow into Hole U1301B. **B.** Calculations of the effective transmissivity ratio (apparent transmissivity/highest transmissivity) as a function of the angle of measurement. Vertical band = orientation of the Site U1301 to Site 1027 experiment, assuming that the direction of highest transmissivity is N20°E (subparallel to the crustal fabric) and the direction of lowest transmissivity is perpendicular to this, N110°E. The orientation of Site 1027 from Site U1301 is N50°E.

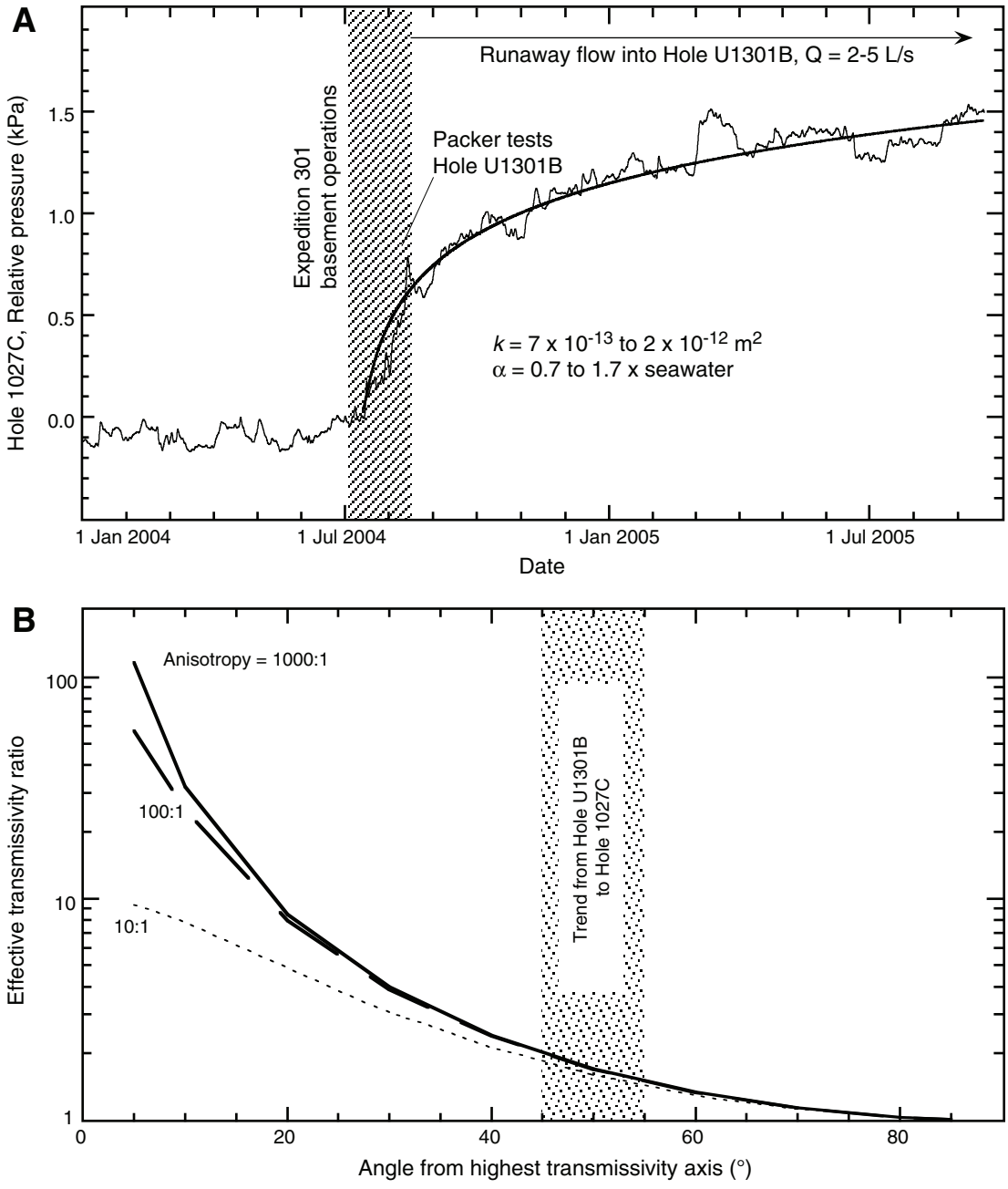

Figure F6. Comparison between near-borehole permeabilities calculated from packer experiments in Hole U1301B (thick, horizontal red bands), those determined in other basement holes from packer (P) and single-hole thermal (flow) (T) experiments, and results of the crosshole experiment (thick, angled red bands). Multiple values and depth intervals shown for packer experiments indicate values calculated based on different thicknesses of tested intervals (Becker and Fisher, 2008). Hole U1301B packer permeabilities are 1–2 orders of magnitude higher than seen at comparable depths at most other sites, except for Hole 839B in the Lau Basin (Bruns and Lavoie, 1994). Hole U1301B packer data indicate higher permeabilities than detected with similar tests shallower in the crust in nearby Holes 1026B and 1027C. The difference between permeability estimated from the crosshole response in Hole 1027C from flow into Hole U1301B and that from packer testing in Hole U1301B might be explained by anisotropy in permeability (and transmissivity) in this area (Fisher et al., 2008). This may also help to explain why permeability estimated from the crosshole experiment is several orders of magnitude lower than that inferred, at a similar crustal scale, based on pressure responses to tidal and tectonic perturbations.